# Electronic Supplementary Material (ESI):

# Facile fabrication of porous Fe@C nanohybrids from natural magnetite as excellent Fischer-Tropsch catalysts

Qian Zhang,[ab] Juwen Gu,[a] Jianfeng Chen,[a] Songbai Qiu*[ab] and Tiejun Wang*[ab]

[a] School of Chemical Engineering and Light Industry, Guangdong University of Technology, Guangzhou 510006, China.

[b] Guangzhou Key Laboratory of Clean Transportation Energy Chemistry, Guangzhou 510006, China.

* Corresponding authors: qiusb@gdut.edu.cn (S. Qiu) and tjwang@gdut.edu.cn (T. Wang)

**Contents**

## 1. Materials and general methods

Three types of natural magnetite used as the starting materials in this work were purchased from Shandong Province Analysis and Test Center (Total iron grade: 62.55%, marked as Natural magnetite-R), Jinan Quandong Institute of Standard Materials (Total iron grade: 69.05%, marked as Natural magnetite-H) and Pangang Group Panzhihua Iron & Steel Research Institute Co., Ltd (Total iron grade: 29.14%, marked as Natural magnetite-L), respectively. The adopted natural magnetite powders were the standard crude ore samples after standard industrial processing and chemical analysis. Herein, the Fe source used for the fabrication of Fe@C nanohybrids is the Natural magnetite-R if not specified. The corresponding chemical compositions of different natural magnetite were listed in Table S1. The chemicals such as ferroferric oxide powder (AR, $Fe_3O_4$), citric acid monohydrate (AR, $C_6H_8O_7 \cdot H_2O$), ammonium hydroxide solution (AR, 25-28%) and silica sand (AR, 80-120 mesh) were purchased from Shanghai Macklin Biochemical Co., Ltd. All reagents and materials were used as received without further purification. The feed syngas of $CO/H_2/N_2$=47.5/47.5/5 in volume ratio with $N_2$ as the internal standard gas for Fischer-Tropsch synthesis (FTS) was supplied by Guangzhou Yuejia Gas Co., Ltd.

The catalysts were analyzed by X-ray diffraction (XRD), X-ray photoelectron spectra (XPS), scanning electron microscopy (SEM), transmission electron microscopy (TEM), $N_2$ adsorption and desorption isotherms and inductively coupled plasma-optical emission spectroscopy (ICP-OES). XRD patterns were recorded by Rigaku SmartLab (3 KW, Japan) with Cu Kα radiation ($\lambda$ = 0.154 nm, Philip) operated at 40 kV and 30 mA. SEM using Hitachi SU8220 (Japan) and TEM using Talos F200S (Czech Republic) were used to study the textural properties and morphologies of the samples. Elemental analysis for the samples was carried out using ICP-OES, Optima 8000, Perkin-Elmer. The X-ray photoelectron spectra (XPS) were carried out by a Leybold LH 10 spectrometer equipped with a single-channel detector, employing Al Kα radiation (1253.6 eV, anode operated at 10 KV × 23 mA). The specific surface area was calculated by the classical BET method at -196.15 $^{o}$C using MicroActive for ASAP 2460 (America), and porosity properties were evaluated by BJH method.

The FTS direct conversion of syngas was carried out in a continuous flow fixed-bed reactor system with a tubular stainless-steel reactor (i.d. 10mm × 350 mm) at 300 $^{o}$C, 2.0 MPa and GHSV of 3000 $ml \cdot g^{-1} \cdot h^{-1}$. For a typical run, 1.0 g catalyst mixed with 2.0 g quartz sands

(80-120 mesh) were loaded into the fixed-bed reactor together. The purpose of mixture operation was to prevent hot spot generation during the exothermic reaction process. Prior to reaction, the loaded catalyst was pre-reduced in situ at 300 $^{o}$C with a syngas flow ($H_2/CO/N_2$=47.5/47.5/5, 50 ml/min) for 12 h at atmospheric pressure, and then cooled down to 100 $^{o}$C. Subsequently, the FTS catalytic reaction was carried out at 300 $^{o}$C and 2.0 MPa with typical time-on-stream of 24 h, and GHSV of 3000 $ml \cdot g^{-1} \cdot h^{-1}$. For the catalytic stability run, time-on-stream of 180 h was proceeded.

During the reaction, gaseous products were analyzed online by gas chromatograph (GC) with TCD and FID detectors. The conversion of CO and $H_2$ was calculated by the $N_2$ internal standard method. The oil products were analyzed offline using Shimadzu QP2010 Plus gas chromatograph-mass spectrometer (GC/MS) equipped with Rts-5MS column (30 m × 0.25 mm × 0.25 um). The column temperature program was as follows: the initial temperature was held at 50 $^{o}$C for 2 min, after that the oven temperature was heated to 150 $^{o}$C with rate of 3 $^{o}$C/min, and then further increased to the final 300 $^{o}$C with rate of 10 $^{o}$C/min and finally held at this temperature for 5 min. The distribution of compositions in oil product was determined based on the relative content of components by peak area normalization[1]. Carbon balance over 90 % was established for all performance runs.

## 2. Synthesis of catalysts

The Fe@C nanohybrids were synthesized through a modified sol-gel approach and the follow-up high-temperature pyrolysis. The corresponding preparation process was shown in Fig. S1. First, certain amount of natural magnetite (or $Fe_3O_4$) and citric acid monohydrate (CA) were mixed in deionized water under continuous stirring, and then the pH value of the solution was adjusted to 3-4 by adding ammonia. In this work, the molar ratio of Fe to CA ranged from 1/1.4-1/3, the molar ratio of 1/1.4 was the biggest Fe/CA ratio that can make sure the fully dissolving of iron in natural magnetite. The dissolution process lasted for 12 h with continuous stirring at about 85 $^{o}$C, then the iron element was effectively extracted from natural magnetite (or $Fe_3O_4$) by complexing with CA to form iron-citrate complex compounds during this process. Subsequently, the insoluble residues in natural magnetite were separated by filtration (no residues when $Fe_3O_4$ was adopted as the starting material). Then the filtrate was gelled gradually by evaporation at 100 $^{o}$C for 72 h in the vacuum oven until dried thoroughly. After that, the fully dried gels were carbonized at 350-900 $^{o}$C for 2h with a heating rate of 10 $^{o}$C/min in $N_2$ flow. Finally, the Fe@C nanohybrids were obtained. For comparison, the Fe@C catalyst prepared from commercial $Fe_3O_4$ was denoted as Fe@C-C-*x*-*y*, where *x* is the molar ratio of Fe/CA which ranged from 1/1.4 to 1/3, and *y* is the carbonization temperature which ranged from 350 to 900 $^{o}$C. Different iron-grading natural magnetite was marked as Natural magnetite-R/H/L, standing for 62.55%, 69.05%, 29.14% Fe contents, respectively. In this work, the Fe source for the preparation of Fe@C nanohybrids was defaulted to the Natural magnetite-R if not specified. For example, the Fe@C-1/1.4-550 catalyst means that the Fe resource is Natural magnetite-R, the Fe/CA molar ratio of starting compositions was 1/1.4, and the carbonization temperature is 550 $^{o}$C.

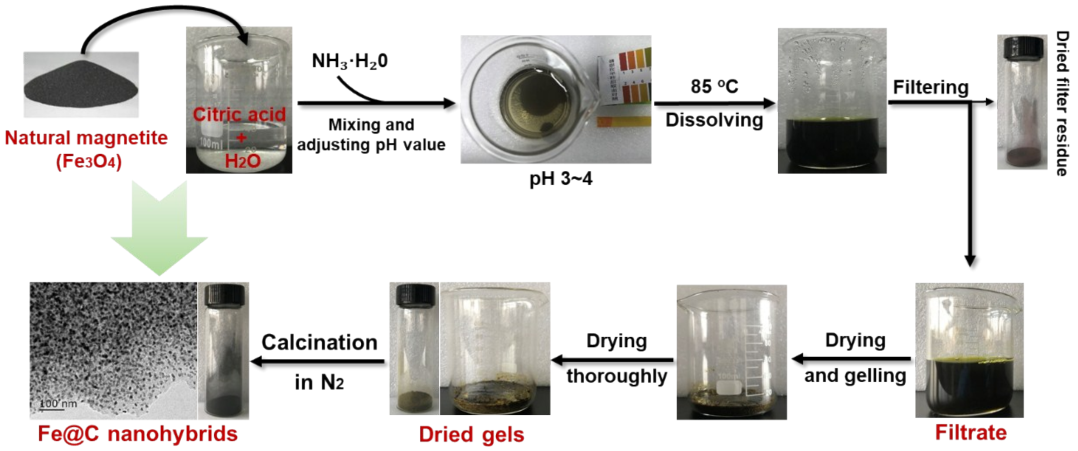

**Fig. S1** Schematic illustration of the green and facile preparation process for the Fe@C nanohybrids derived from natural magnetite.

The porous $Fe_3O_4$ microspheres (FeMs) were synthesized by a hydrothermal synthesis approach[2]. Typically, $FeCl_3·6H_2O$ (1.35 g) was dissolved in ethylene glycol (40 mL) to form a clear solution. Then sodium acetate (3.6 g) was added to the solution under vigorous stirring. Subsequently, a homogeneous mixture solution was obtained. After stirring vigorously for 30 min, the mixture was sealed into a Teflon-lined stainless-steel autoclave (100 ml). The hydrothermal process was processed at 200 $^{o}$C for 12 h, after that the autoclave was naturally cooled to room temperature. The desired FeMs products were separated by magnetism and washed several times with deionized water and ethanol. Then, the obtained black products were dried at 60 $^{o}$C in a vacuum drying oven for 12 h. Finally, the obtained black powder was denoted as FeMs.

For comparison, the commercially available Natural magnetite-R from Shandong Province Analysis and Test Center was also used for the FTS directly without further purification.

## 3. Catalyst Characterizations

**Table S1** Chemical compositions of the natural magnetite precursors, the dissolution residues and the as-prepared Fe@C nanohybrids.

| Samples | Source | Chemical compositions (wt%) |
|---|---|---|
| Natural magnetite-R | Shandong Province Analysis and Test Center (No. 93-94) | Totle iron grade (TFe): 62.55 %.<br>FeO 25.30 %, $SiO_2$ 3.20 %, $Al_2O_3$ 0.59 %, CaO 1.50 %, MgO 3.04 %, $K_2O$ 0.054 %, $Na_2O$ 0.026 %, $TiO_2$ 0.041 %, Mn 0.11 %, S 2.94 %, P 0.017 %. |
| Natural magnetite-H | Jinan Quandong Institute of Standard Materials (No. QD 10-121) | Totle iron grade (TFe): 69.05 %.<br>MgO 0.17%, FeO 23.8%, MnO 0.079%, $SiO_2$ 2.45%, $TiO_2$ 0.313%, $Al_2O_3$ 0.50%, P 0.010%, CaO 0.2%, S 0.011%. |
| Natural magnetite-L | Pangang Group Panzhihua Iron & Steel Research Institute Co., Ltd. (No. YSBC19726-2014) | Totle iron grade (TFe): 29.14 %.<br>MgO 6.72%, FeO 21.09%, MnO 0.288%, $SiO_2$ 23.12%, $TiO_2$ 10.36%, $Al_2O_3$ 8.83%, P 0.011%, CaO 7.27%, S 0.656%, $V_2O_5$ 0.268%. |
| Residue-R | Natural magnetite-R | Fe: 53.66 %, $SiO_2$ 4.31 %, $Al_2O_3$ 0.92%, CaO 2.76 %, MgO 4.64 %, $K_2O$ 0.11 %, $Na_2O$ 0.22 %, $TiO_2$ 0.046 %, Mn 0.11 %, S 3.71 %, P 0.021 %, $V_2O_5$ 0.0054 % |
| Residue-H | Natural magnetite-H | Fe: 58.65%, $SiO_2$ 5.65 %, $Al_2O_3$ 1.16%, CaO 0.54 %, MgO 0.39 %, $K_2O$ 0.1 %, $Na_2O$ 0.39 %, $TiO_2$ 0.48 %, Mn 0.062 %, S 0.02 %, P 0.013 %, $V_2O_5$ 0.082 % |
| Residue-L | Natural magnetite-L | Fe: 17.79 %, $SiO_2$ 28.85 %, $Al_2O_3$ 11.02%, CaO 8.77 %, MgO 8.10 %, $K_2O$ 0.11 %, $Na_2O$ 1.28 %, $TiO_2$ 12.93 %, Mn 0. 0.26 %, S 0.36 %, P 0.01 %, $V_2O_5$ 0.13 % |

| | | |
|---|---|---|
| Fe@C-1/1.4-900 | Natural magnetite-R | Fe 64.31 %, others: C 30.53 %, Si 0.91 %, Al 0.11 %, Ca 0.21 %, Mg 0.72 %, K 0.020 %, Na 0.048 %, Ti 0.022 %, P <0.0020 %, S 0.37 %, Mn 0.25 %. |

**Table S2** The Fe element utilization efficiency of different natural magnetite precursors.

| Precursor | Weight (g) / Fe (wt%) in raw precursor | Weight (g) / Fe (wt%) in dissolution residue | $UE_{Fe}$ (%) [a] |
|---|---|---|---|
| Natural magnetite-R | 6.0438 / 62.55 [b] | 2.2810 / 53.66 | 67.6 |
| Natural magnetite-H | 5.4294 / 69.05 % | 1.9867 / 58.65 | 68.9 |
| Natural magnetite-L | 12.7935 / 29.14 % | 9.2236 / 17.79 | 56.0 |

[a] The utilization efficiency of Fe element.

[b] The Fe content results were gained by ICP-OES analysis.

The utilization efficiency of Fe element ($UE_{Fe}$) from different natural magnetite in the facile preparation process for the Fe@C nanohybrids was calculated based on the mass and Fe content of the natural magnetite precursor and the insoluble residue as the equation below:

$$UE_{Fe}(\%) = \left[1 - \left(m_{residue} \times Fe_{residue} wt\%\right) / \left(m_{precursor} \times Fe_{precursor} wt\%\right)\right] \times 100\%$$

The results revealed that the Fe elements utilization efficiency could reach to 67.6 %, 68.9 % and 56.0 % with Natural magnetite-R, Natural magnetite-H and Natural magnetite-L as the precursor, respectively.

**Table S3** Textural properties of the samples.

| Samples | Fe/CA molar ratio | $S_{BET}$ ($m^2/g$)[a] | Pore volume ($cm^3/g$)[a] | Average pore diameter (nm)[a] |
|---|---|---|---|---|
| Natural magnetite-R | - | 0.2 | 0.0036 | 54.9 |
| $Fe_3O_4$-Commercial | - | 3.2 | 0.018 | 40.4 |
| FeMs | - | 20.2 | 0.05 | 23.9 |
| Fe@C-1/1.4-550 | 1/1.4 | 73.4 | 0.10 | 3.9 |
| Fe@C-1/1.4-900 | 1/1.4 | 157.7 | 0.35 | 6.6 |

[a] Surface area, pore volumes and diameters of the samples were calculated using standard BET and BJH theory, respectively.

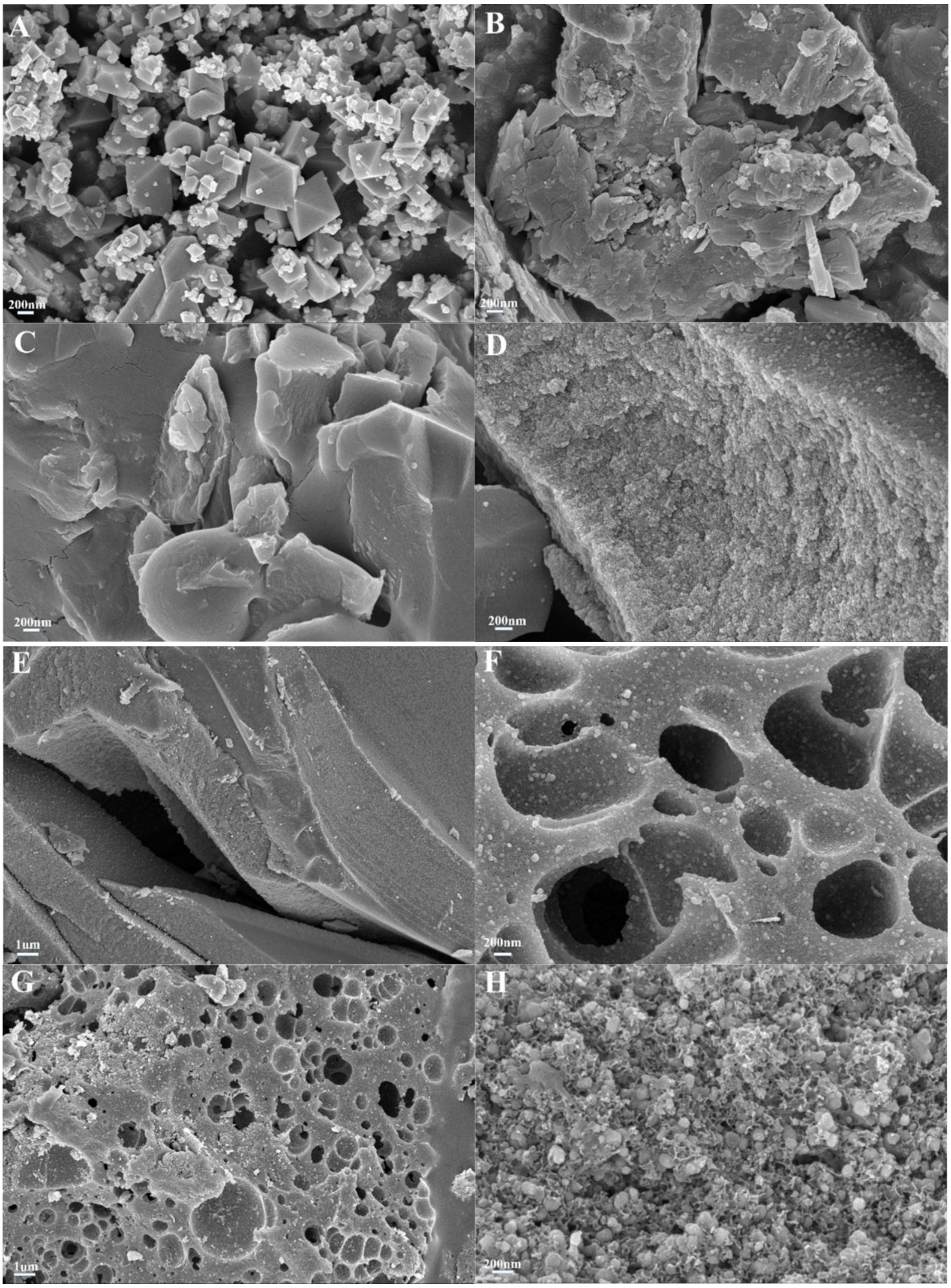

**Fig. S2** SEM imagines of $Fe_3O_4$-commercial (A), natural magnetite-R (B), the precursor of dried gels (C), and the as-prepared Fe@C-1/1.4-450 sample (D), Fe@C-1/1.4-550 sample (E), Fe@C-1/1.4-700 sample (F), and Fe@C-1/1.4-900 sample (G and H).

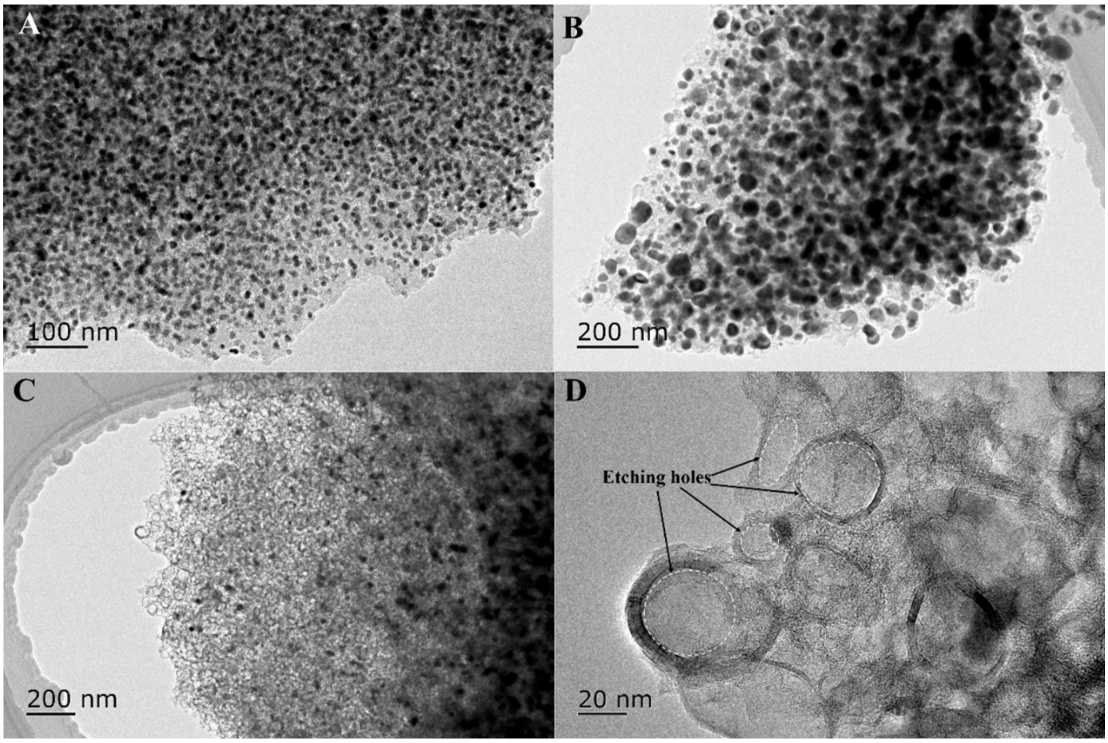

**Fig. S3** TEM images of the Fe@C-1/1.4-550 sample (A) and Fe@C-1/1.4-900 sample (B), and the corresponding acid treated Fe@C-1/1.4-900 sample (C and D). (Acid-treatment conditions: the solid sample was washed five times with 10.0 wt% $H_2SO_4$ at 85 $^oC$ for 12 h to remove unwrapped iron species, then the residue was washed with deionized water)

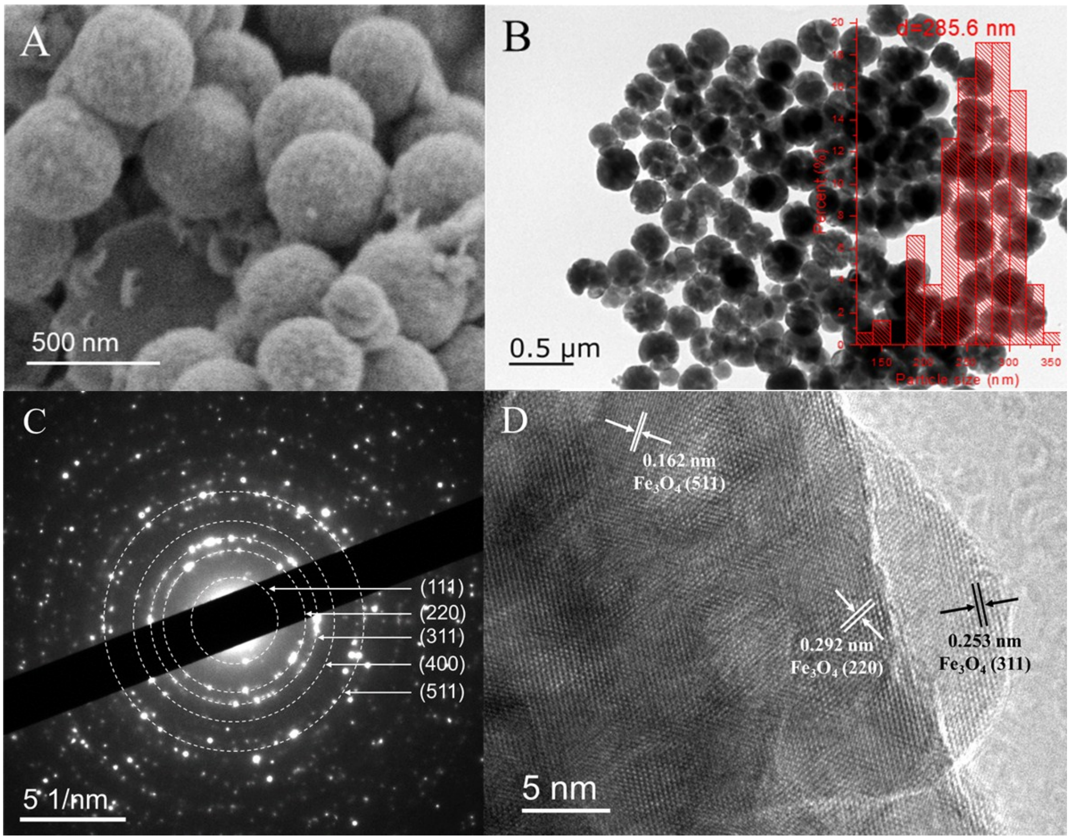

**Fig. S4** SEM (A), TEM (B), SAED patterns (C) and HRTEM (D) of the prepared FeMs.

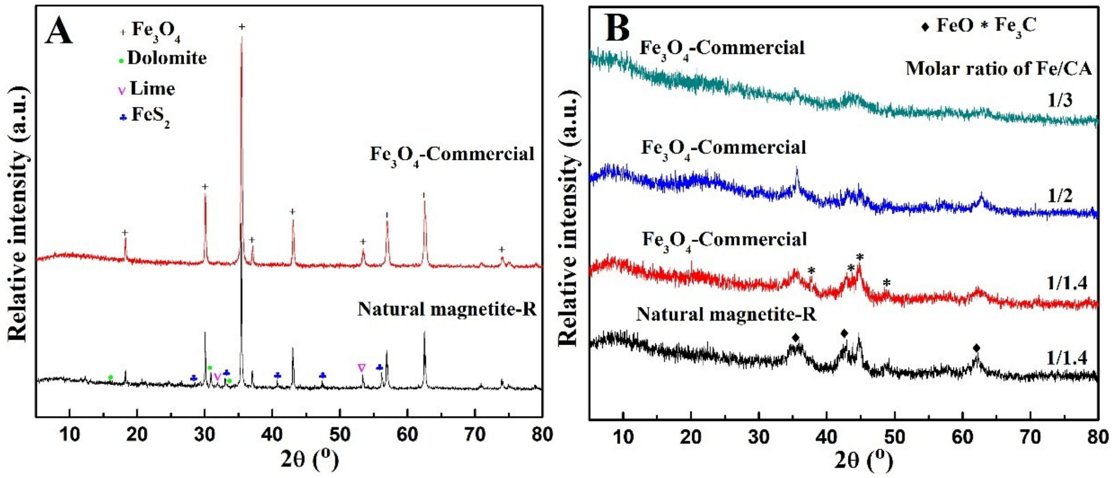

**Fig. S5** XRD patterns of the commercial $Fe_3O_4$ and Natural magnetite-R (A), Fe@C nanohybrids prepared with different precursor and Fe/CA molar ratio at carbonization temperature of 550 $^oC$ (B).

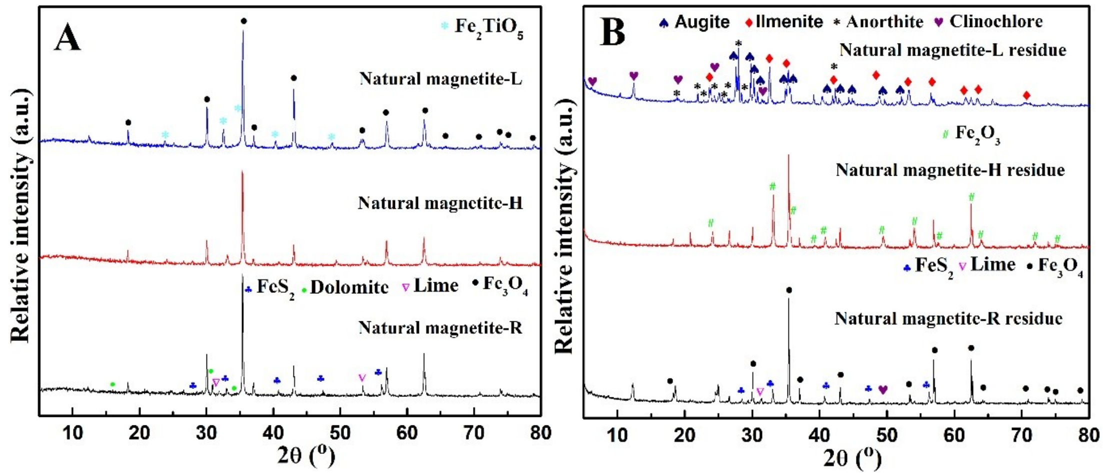

**Fig. S6** XRD patterns of the different kinds of natural magnetite (A) and corresponding dissolution residues (B).

The XRD patterns of different kinds of natural magnetite and the corresponding insoluble residues were further analyzed as shown in Fig. S6. The natural magnetite can't be dissolved thoroughly by citric acid (CA) due to the existence of mineral impurities except $Fe_3O_4$. In Fig. S6B, the insoluble phases of augite (JCPDS No. 024-0203), ilmenite (JCPDS No. 005-0778), anorthite (JCPDS No. 018-1202), clinochlore (JCPDS No. 029-0701) and $Fe_2O_3$ (JCPDS No. 033-0664) were detected except $Fe_3O_4$ (JCPDS No. 019-0629). The appearance of $Fe_2O_3$ could ascribed to the oxidation of $Fe_3O_4$ constituent during dissolution.

## 4. Catalytic activities

**Table S4** FTS catalytic activities of different catalysts.

| Catalyst | Precursor | Conversion (%) | | Selectivity of $CO_2$ (C%) | Oil yield (C%) | Hydrocarbon selectivity (wt%, free of $CO_2$) | | | C2-4 O/P [c] | α- Chain growth probability factor [a] |
|---|---|---|---|---|---|---|---|---|---|---|
| | | CO | $H_2$ | | | C1 | C2-4 | C5+ | | |
| Natural magnetite-R | - | 6.8 | 14.7 | 17.7 | -[b] | 84.1 | 15.9 | - | 0.1 | 0.167 |
| FeMs | $FeCl_3 \cdot 6H_2O$ | 61.4 | 60.7 | 38.2 | 11.9 | 15.8 | 36.0 | 48.2 | 2.4 | 0.808 |
| $Fe_3O_4$-Commercial | - | 68.1 | 56.0 | 35.2 | 18.3 | 11.8 | 27.7 | 60.5 | 2.6 | 0.830 |
| Fe@C-C-1/1.4-550 | $Fe_3O_4$-Commercial | 78.5 | 62.8 | 38.8 | 12.7 | 16.1 | 37.8 | 46.1 | 1.5 | 0.824 |
| Fe@C-C-1/2-550 | | 71.4 | 61.3 | 40.3 | 9.1 | 22.1 | 36.4 | 41.5 | 1.5 | 0.824 |
| Fe@C-C-1/3-550 | | 80.9 | 70.2 | 37.3 | 7.43 | 37.9 | 37.0 | 25.1 | 0.9 | 0.761 |
| Fe@C-1/1.4-350 | Natural magnetite-R | 16.6 | 24.8 | 10.3 | - | 61.9 | 38.1 | - | 1.3 | 0.348 |
| Fe@C-1/1.4-450 | | 35.0 | 39.7 | 34.5 | - | 48.3 | 50.2 | 1.5 | 1.2 | 0.320 |
| Fe@C-1/1.4-550 | | 76.5 | 59.3 | 37.3 | 10.6 | 17.6 | 39.6 | 42.8 | 1.3 | 0.815 |
| Fe@C-1/1.4-600 | | 91.0 | 77.7 | 40.3 | 11.6 | 35.5 | 40.9 | 23.6 | 0.5 | 0.761 |
| Fe@C-1/1.4-700 | | 96.8 | 81.6 | 34.9 | 15.3 | 27.2 | 36.7 | 36.1 | 0.6 | 0.780 |
| Fe@C-1/1.4-800 | | 96.8 | 79.8 | 36.2 | 18.0 | 24.8 | 35.2 | 40.0 | 0.9 | 0.779 |
| Fe@C-1/1.4-900 | | 98.6 | 81.4 | 38.1 | 21.6 | 17.6 | 31.8 | 50.6 | 1.5 | 0.778 |
| Fe@C-H-1/1.4-900 | Natural magnetite-H | 98.3 | 77.1 | 40.8 | 23.2 | 16.4 | 31.9 | 51.7 | 2.5 | 0.777 |
| Fe@C-L-1/1.4-900 | Natural magnetite-L | 97.7 | 78.0 | 39.6 | 15.5 | 25.6 | 39.8 | 34.6 | 0.7 | 0.703 |

[a] According to the Anderson-Schulz-Flory distribution and Schulz formula: $\ln(W_n/n) = n \ln\alpha + \ln((1-\alpha)^2/\alpha)$, the selectivity of heavy hydrocarbon increased with the increase of α.

[b] No oil product collected after the 24 h FTS reaction.

[c] O/P means the ratio of olefin to paraffin.

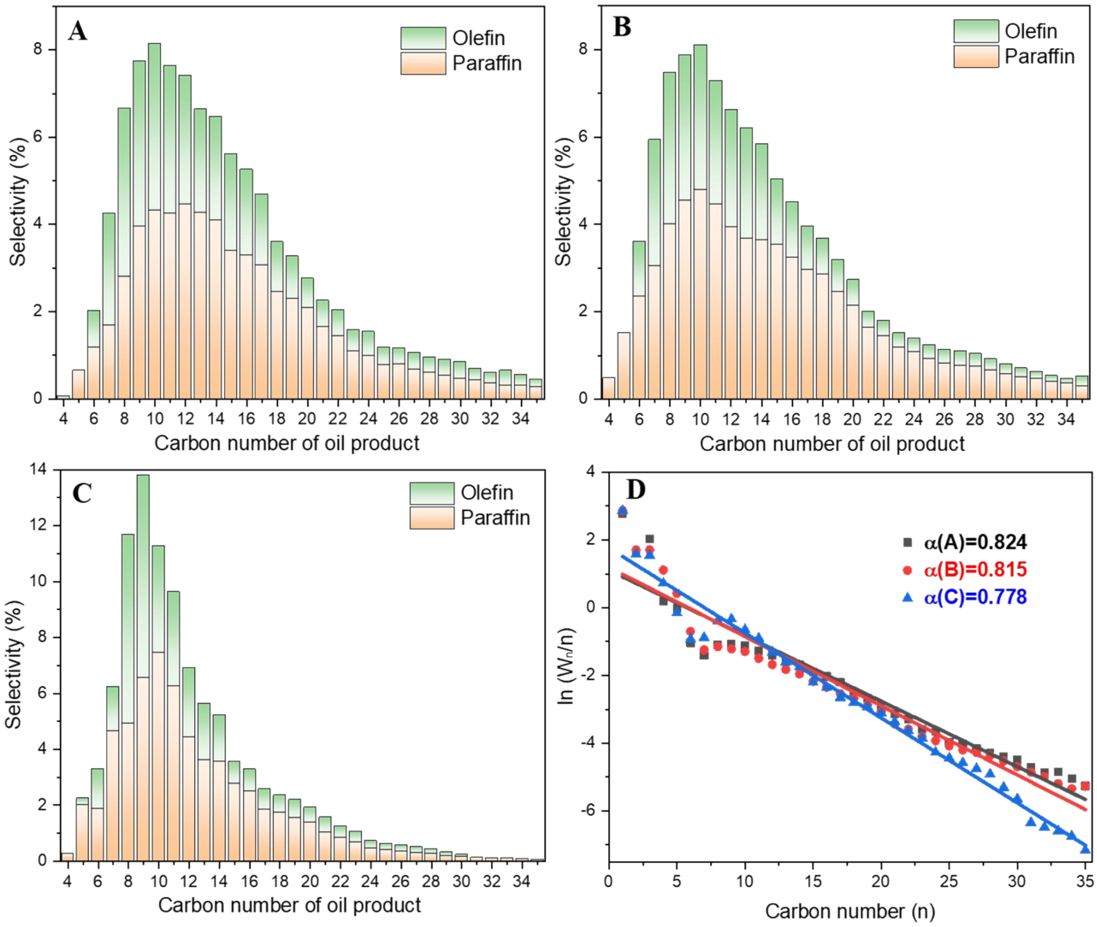

**Fig. S7** Carbon distribution of oil product in FTS catalyzed by Fe@C-C-1/1.4-550 (A), Fe@C-1/1.4-550 (B), Fe@C-1/1.4-900 (C) and the Anderson-Schulz-Flory distribution of products (D) (Chain growth probability factor is generated from the Schulz formula: $\ln(W_n/n) = n \ln\alpha + \ln((1-\alpha)^2/\alpha)$, n is the carbon number of hydrocarbons and $W_n$ is the mass ratio of hydrocarbons with carbon number n).[3, 4]

## References

1. Z. Sun, S. Toan, S. Y. Chen, W. G. Xiang, M. H. Fan, M. Zhu and S. W. Ma, *Int J Hydrogen Energ*, 2017, **42**, 16031-16044.
2. Y. L. Zhang, L. L. Ma, T. J. Wang and X. J. Li, *Catal Commun*, 2015, **64**, 32-36.
3. A. Tavakoli, M. Sohrabi and A. Kargari, *Chem Eng J*, 2008, **136**, 358-363.
4. J. Li, Y. L. He, L. Tan, P. P. Zhang, X. B. Peng, A. Oruganti, G. H. Yang, H. Abe, Y. Wang and N. Tsubaki, *Nat Catal*, 2018, **1**, 787-793.